# Computer Simulations of Dense-Branching Patterns

J. Erlebacher, P. C. Searson, and K. Sieradzki
*Department of Materials Science and Engineering, The Johns Hopkins University, Baltimore, Maryland 21218*
(Received 2 July 1993)

We present a novel Monte Carlo simulation of electrochemical deposition that shows a smooth transition between diffusion limited aggregation and dense-branching morphology. The essential element of the simulation is to divide the growth field into two areas, a "space charge" region surrounding the aggregate in which particle motion is biased to branch tips, and a second region surrounding the first in which particle motion follows unbiased random walks. The interface between these areas is stable to perturbations of wavelength smaller than the size of the space charge region.

PACS numbers: 61.50.Cj, 02.70.Lq, 68.70.+w

Electrochemical deposition of branched aggregates has been extensively studied in the last ten years, both by experiment and computer simulation [1]. Experimentally, deposits can be formed in a thin layer cell in radial configuration where deposition is initiated at a point cathode located at the center of a circular anode. Aggregates are deposited from an unsupported electrolyte. Depending on the electrolyte concentration and deposition voltage (or current), the aggregates may exhibit a number of characteristic growth patterns such as diffusion limited aggregation (DLA), dense-branching morphology (DBM), and dendritic morphologies. These gross morphologies have been extensively studied for copper and zinc deposits [2–4] and have also been reported in the electrodeposition of conducting polymers [5].

At low voltages and low electrolyte concentrations, treelike structures are obtained that exhibit many of the characteristics of the DLA model of Witten and Sander [6]. At higher voltages and electrolyte concentrations, a growth transition is observed to DBM. This morphology is characterized by a high aggregate density and a smooth growth front. At even higher voltages, dendritic aggregates appear in which crystalline anisotropy manifests itself on the longest length scales. In this paper we focus on the DLA and DBM morphologies. DBM has been of particular interest due to the apparent smoothness and stability of the growth front. It has been thought, in analogy to temperature and concentration gradients in solidification processes, that the coupled diffusion and electric fields in the electrolyte solution would lead to a Mullins-Sekerka instability in the growth front [7,8].

Recent work [9–11] has confirmed predictions of a space charge layer around the aggregate. These groups have concluded that transport in the electrolyte to the growing deposit can be divided into two regions. The first region, close to the deposit, is the space charge region, where a high electric field and large concentration gradient exist. The second region, in the bulk of the electrolyte, is a region of negligible concentration gradient and low field. This partitioning has been shown to be an excellent approximation to the coupled diffusion and electromigration transport in the cell [10,11]. The simplest way to implement this in a simulation is to allow ballistic transport of particles near the aggregate fed by a flux of particles arriving via transport through a Laplacian field existing over most of the cell area.

In this Letter, we present a novel Monte Carlo simulation for electrochemical deposition of branched aggregates in which the transport of the metal cations is diffusion controlled in the region far from the aggregate and migration controlled in the space charge region close to the aggregate. Patterns generated using this model confirm the importance of migrational transport in DBM. A smooth transition from DLA to DMB is found by varying the width of the migrational zone and the particle concentration, which control the length scale of the perturbations in the growth front. We find that a radial growth front is stabilized when the wavelength of perturbations on the interface between the diffusional and migrational regions is smaller than the size of the space charge region. Formally, this approach considers the driving force for deposition to be a gradient in electrochemical potential giving rise to coupled diffusion-electromigration transport. Our simulations approximate the steady-state solution to the Nernst-Planck equation with no convection term.

In this model, particles are launched from a circle far from the growing aggregate, representing the symmetry of the Laplace field as determined by the anode. The mechanics of this part of the simulation are identical to DLA and represent the motion of particles over the greater area of an electrochemical cell. When particles reach a distance, $L$, from the aggregate (Fig. 1), entering the space charge region, they are then transported along straight line trajectories to the closest point on the aggregate. The distance $L$ is measured normal to an envelope following the contour of the aggregate. The migrational envelope was modeled as a closed line defined by a series of nodes. Initially, the aggregate is seeded by a single particle representing a point cathode, and the migrational envelope is a circle with radius $L$ centered at this point.

This model has two important differences to the Witten and Sander model. First, the migration length $L$ repre-

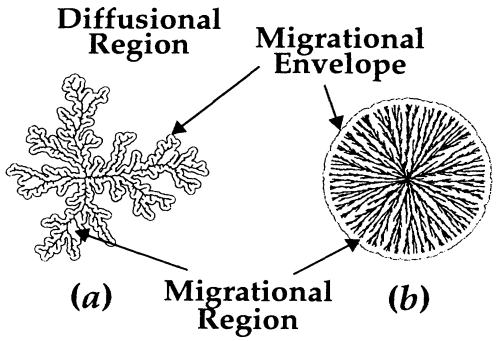


FIG. 1. Typical (a) DLA and (b) DBM aggregates showing migrational and diffusional regions. In (a) $L=10$, $J\approx 0$; 10000 nodes, 5000 particles. In (b) $L=10$, $J=0.5$; 4500 nodes, 25262 particles.

sents the distance over which migration is the dominant transport process. In electrodeposition experiments, $L$ is dependent on the electrolyte concentration and applied voltage in the cell. Second, a concentration is simulated by launching a given number of particles, $J$, per unit length of the migrational envelope on each Monte Carlo iteration, corresponding to a constant particle flux [12]. Radial density profiles indicate that a constant aggregate density is maintained for simulated DBM aggregates. During the simulation, the shape of the migrational envelope is dynamically maintained around the growing aggregate. Note that the migrational envelope construction contains no *a priori* assumptions about the ultimate aggregate geometry.

A Monte Carlo (MC) iteration was defined by the following steps:

(i) The perimeter $P$ of the migrational envelope is measured by summing the distances between the nodes. The number of particles to be incorporated in the aggregate per iteration is given by $JP$. As the aggregate grows, the perimeter of the migrational envelope increases, and the corresponding number of particles launched per iteration also increases.

(ii) A random walker is launched in the diffusional region from a virtual circle that completely surrounds the aggregate. The motion of the random walker is off lattice and controlled by common DLA algorithms [13,14].

(iii) The walker continues on its path until it passes through the migrational envelope, at which point its coordinate is translated along the line to the nearest particle on the interface of the growing aggregate so that they touch. The coordinate of the particle is saved but not added to the list of coordinates that comprise the aggregate until step (v).

(iv) Steps (ii) and (iii) are repeated for the number of particles determined in step (i). Note that the coordinates saved in step (iii) do not influence the motion of other particles launched in the same MC iteration, so that there exists the possibility that particles launched in the same iteration may partially overlap. This approach to multiparticle aggregation is different than keeping track of large ensembles of nonoverlapping random walkers typically used in multiparticle diffusion limited aggregation studies [15–18].

(v) The coordinates collected in step (iii) are added to the coordinates that comprise the aggregate. The nodes that comprise the migrational envelope are repositioned so that the migrational envelope at every point is the distance $L$ away from the aggregate.

Figure 2 shows a morphological structure map of patterns produced using this algorithm with $L$ ranged from 2 to 50 units and $J$ ranged from 0 to 0.5 (particle/unit length)/iteration. $J\approx 0$ corresponded to a single particle being launched in an iteration, regardless of aggregate or envelope size. Particles had a diameter of 1, and all aggregates were grown to a diameter of about 400 units, with masses in the range of 4000 to 50000 particles. Typically, between 3000 and 10000 nodes were used to define the migrational envelope.

Inspection of Fig. 2 shows that patterns generated by this model are very similar to electrodeposited aggregates, transforming in a continuous manner from DLA to DBM as the concentration and migration lengths are increased. When the concentration is small and the migration length is short, the model is most similar to the Witten and Sander model. Measurement of the fractal dimension of the $L=2$, $J\approx 0$ aggregate by a simple mass-radius measurement yielded a fractal dimension of 1.68, near the expected value of 1.71 [13]. We further note that increasing the migration length reduces the smaller length scale features in the deposits, so that at low concentrations and high migration lengths, the aggregates are similar to the "stringy" deposits grown experimentally at low concentrations and high voltages [2]. The morphological trends shown in Fig. 2 are consistent with experimental observation if the migration length is related to the voltage and concentration by an expression of the form $L\propto(V/C^{\beta})^{\alpha}$, as has been suggested [8]. As a result, each column of Fig. 2 represents a set of aggregates produced by modifying the analog of a voltage, and as the voltage is increased, sidebranching is decreased. Modification of the electrolyte concentration does not simply correspond to translation along a row or column in Fig. 2 since both axes are dependent on this parameter. No sharp discontinuities were observed in the growth velocities, consistent with the structure map.

An essential feature of this model for generating dense-branching aggregates is to allow particles that are launched in the same Monte Carlo iteration to overlap. We have also grown two-dimensional off-lattice aggregates in which particle overlap is not allowed, and although for certain sets of conditions the stability of the migrational envelope is maintained, the deposits are not realistically dense. We found that by allowing particle overlap, we could reduce the branch split angle from 60°, the minimum possible when packing nonoverlapping cir-

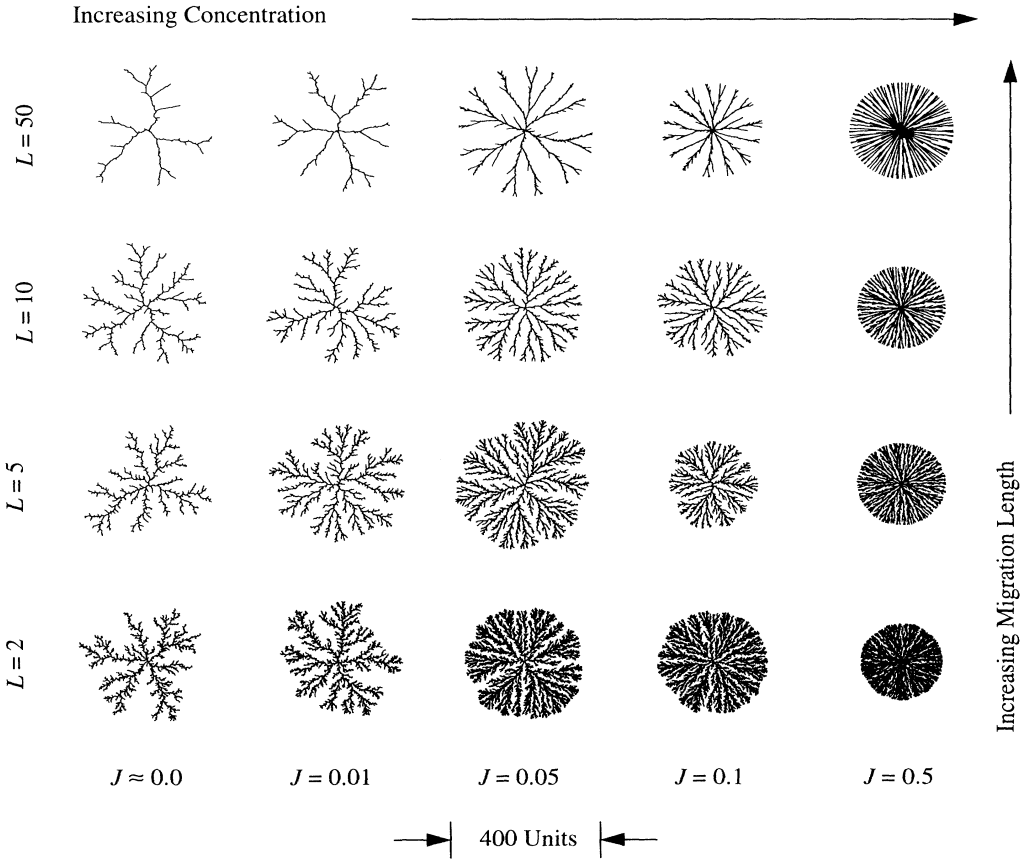


FIG. 2. Structure map of simulated electrodeposited aggregates, showing morphological variation with migration length $L$ and concentration $J$.

cular particles, and thereby increase aggregate density. It is suggested that particle overlap and smaller branching angles introduce a degree of three dimensionality to the growth of the aggregates, extending the $J,L$ values over which the dense-branching morphology is seen. We note that experimental dense-branching deposits grown in thin layer cells are obtained from cells at least 100 $\mu$m in thickness [2–4].

We now suggest a stability criterion for the radially symmetric migrational envelopes of DBM aggregates, based on an analysis of an arc $s$ on the migrational envelope supplying particles to a single branch tip, illustrated in Fig. 3. The migrational envelope will be stable if the number of particles attaching to that tip during an iteration, $sJ$, uniformly push the envelope back into the diffusive region. That is, the arc angle $\theta = s/L$ is maintained if at least $sJ$ particles can uniformly distribute over the base of the sector defined by $s$ and $\theta$. Since the particle diameter is 1, $\theta \approx sJ$, so that a stability criterion for that section of the migrational envelope is $LJ \geq 1$. This stability criterion expressed in terms of the average perturbation wavelength $\lambda$ is $\lambda/L \leq 1$, where $\lambda \equiv 1/J$. Thus, at constant $J$ and for increasing $L$, longer wavelength perturbations can be sustained while maintaining the stability of the envelope.

In conclusion, we present a Monte Carlo computer simulation for electrochemical deposition that produces the range of aggregate morphologies from DLA to DBM

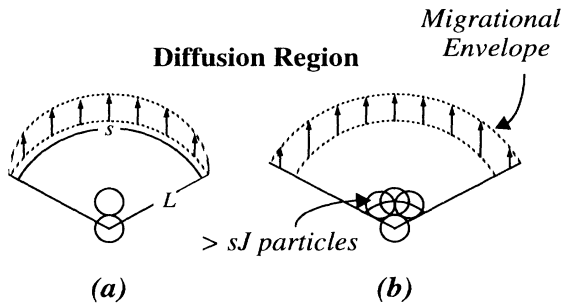


FIG. 3. Geometric construction showing (a) unstable, $JL < 1$, and (b) stable, $JL \geq 1$, branch propagation. It is suggested that the aggregate is stable when the migrational envelope is uniformly pushed into the diffusion region, which occurs when the flux of aggregating particles fills the base of the arc defined by $s$ and $L$.

in a physically significant way. The model does not incorporate crystal anisotropy and curvature effects, which are thought to influence dendritic growth. To generate the DLA to DBM transition, our simulations incorporate the construction of a migrational envelope surrounding a growing aggregate within which particle motion is biased toward the nearest point on the aggregate. Outside the migrational envelope, the transport of ions is diffusive. These regions correspond to recent experimentally observed and theoretically predicted models of electrodeposition. The stability of envelopes surrounding dense-branching deposits is a natural result of aggregating particles spreading out over the tips of growing branches.

We would like to acknowledge useful discussions with P. Meakin during the initial stages of this work and support of this work by the National Science Foundation under Grant No. DMR 9202645.

[1] E. Ben-Jacob, and P. Garik, Nature (London) **343**, 523 (1990).
[2] Y. Sawada, A. Dougherty, and J. P. Gollub, Phys. Rev. Lett. **56**, 1260 (1986).
[3] D. Grier, E. Ben-Jacob, R. Clarke, and L. M. Sander, Phys. Rev. Lett. **56**, 1264 (1986).
[4] D. Barkey, P. Garik, E. Ben-Jacob, B. Miller, and B. Orr, J. Electrochem. Soc. **139**, 1044 (1992).
[5] M. Fujii, K. Arii, and K. Yoshino, J. Electrochem. Soc. **140**, 1838 (1993); M. Fujii and K. Yoshino, Jpn. J. Appl. Phys. **27**, L457 (1988).
[6] T. A. Witten and L. M. Sander, Phys. Rev. Lett. **47**, 1400 (1981); Phys. Rev. B **27**, 5686 (1983).
[7] W. W. Mullins and R. F. Sekerka, J. Appl. Phys. **35**, 444 (1964).
[8] D. Grier, D. Kessler, and L. M. Sander, Phys. Rev. Lett. **59**, 2315 (1987).
[9] V. Fleury, M. Rosso, J.-N. Chazalviel, and B. Sapoval, Phys. Rev. A **44**, 6693 (1991).
[10] J.-N. Chazalviel, Phys. Rev. A **42**, 7355 (1990).
[11] J. R. Melrose, D. B. Hibbert, and R. C. Ball, Phys. Rev. Lett. **65**, 3009 (1990).
[12] In the radial geometry, the experimental analog of constant particle flux occurs at constant voltage growth conditions for fixed anion concentration during steady-state growth.
[13] S. Tolman and P. Meakin, Phys. Rev. A **40**, 428 (1989).
[14] P. Ossadnik, Physica (Amsterdam) **176A**, 454 (1991).
[15] R. Voss, J. Stat. Phys. **36**, 861 (1984).
[16] P. Meakin, Physica (Amsterdam) **153A**, 1 (1988).
[17] T. Nagatani, Phys. Rev. A **46**, 2022 (1992).
[18] M. Uwaha and Y. Saito, Phys. Rev. A **40**, 4716 (1989).